

## SYNTHESIS OF PHOTOLUMINESCENT PURE AND DOPED CADMIUM SULFIDE BY REVERSE MICROEMULSION METHOD

A. I. IORGU, D. BERGER, L. ALEXANDRESCU, B. S. VASILE, C. MATEI\*  
*Department of Inorganic Chemistry, Physical Chemistry and Electrochemistry,  
University "POLITEHNICA" of Bucharest, 1-7 Polizu street, Bucharest 011061,  
Romania*

Nanomaterials with controlled morphology have drawn significant attention due to their unique optical, electrical and chemical properties originating from their quantum size. The reverse microemulsion method is one of the most recognized soft chemistry routes for the synthesis of nanocrystals with very narrow size distribution. We report on the synthesis of photoluminescent cadmium sulfide nanoparticles doped with different ions ( $\text{Ag}^+$ ,  $\text{Mn}^{2+}$ ,  $\text{Zn}^{2+}$ ) by reverse microemulsion method. The structure and morphology of the samples were investigated by X-ray diffraction, scanning and transmission electron microscopy. The optical characterization of colloidal systems was carried out by UV-vis and photoluminescence (PL) spectroscopy. Different photoluminescent properties were obtained by varying the doping ion and its content.

(Received October 15, 2013; November 29, 2013)

**Keywords:** Reverse microemulsion method, Photoluminescence, Pure and doped CdS

### 1. Introduction

Many advances in the field of nanomaterials led to the obtaining of high quality semiconductor nanocrystals, which exhibit unique optical, physical and chemical properties owing to their quantum size and surface effects. Light emission from semiconductor nanocrystals is possible through a recombination process of charge carriers produced by photon absorption. The emission wavelength can be tuned by controlling nanocrystals size during the synthesis [1, 2]. The nanomaterials with photoluminescent properties are considered as luminophors for displays, bio-labels, lasers, etc. [3, 4]. One of the most studied photoluminescent nanomaterial is cadmium sulfide, a typical II-VI-type semiconductor with a band gap of 2.4 eV at room temperature, having a wide range of applications, such as solar cells, laser diodes, photocatalysts, photovoltaics, etc. [5-7]. Recently, the photoluminescence of pure or doped cadmium sulfide was extensively studied for optical biosensor applications [8]. Moreover, it was found that surface plasmon induced photoluminescence [9] is a very sensitive technique to detect ultralow concentrations of biological species [10]. Electroluminescent CdS-based systems, with enhanced electrochemiluminescence achieved by interaction with surface plasmon of gold nanoparticles, were tested for ultrasensitive detection of thrombin [11], low-density lipoprotein [12] and DNA [13]. These electroluminescent systems have the advantage of a facile integration into microelectronic devices with addressable ports for simultaneous detection of different biologic species.

The increasing interest for nanostructured materials led to a wide range of synthesis approaches, like precipitation in the presence of a template agent (a surfactant or a polymer), reverse microemulsion method, solvothermal synthesis, etc. For cadmium sulfide nanocrystals with various morphologies, many synthesis methods were reported [14]. Among these, the reverse microemulsion method has many advantages as it does not imply high temperatures or expensive equipment and the crystal growth can be very well controlled by varying the reaction conditions and the microemulsion parameters [15-17]. The reverse microemulsion is heterogeneous on a

---

\* Corresponding author: cristi\_matei@yahoo.com

molecular scale, but thermodynamically stable, representing a suitable reaction media for nanoparticles synthesis, since water droplets act as nanoreactors, which favor the formation of small individual crystals with a narrow size distribution [18].

Doping cadmium sulfide has attracted a lot of attention as it is a convenient way to tailor its physical properties. Many reports are available in literature regarding the doping effect on metallic chalcogenides [19-21], proving that the photoluminescent and electrical features of sulfide nanocrystals can be easily tuned [5]. Still, on our best knowledge, no comparative analysis on the influences of different dopant ions on cadmium sulfide properties has been performed. To study the effect of doping ion on the photoluminescence of cadmium sulfide we chose an appropriate method for the synthesis of nanoparticles with controlled morphology, as the properties of material depend sensitively on both size and shape of particles. Therefore, we report here the obtaining of pure and doped cadmium sulfide nanocrystals by reverse microemulsion approach and the influence of various dopant ions like  $\text{Ag}^+$ ,  $\text{Mn}^{2+}$  and  $\text{Zn}^{2+}$  on its photoluminescent properties. In order to investigate the influence of doping ion, the reaction conditions and microemulsion parameters were kept constant in all samples preparation.

## 2. Experimental

All metallic sulfides were prepared by double reverse microemulsion method. Metallic chlorides or acetates and sodium sulfide (Sigma-Aldrich, 99%) were used as 0.2 M aqueous solutions. All chemicals ( $\text{Cd}(\text{CH}_3\text{COO})_2 \cdot 2\text{H}_2\text{O}$ ,  $\text{Zn}(\text{CH}_3\text{COO})_2 \cdot 2\text{H}_2\text{O}$ ,  $\text{ZnCl}_2$ ,  $\text{CdCl}_2 \cdot 2.5\text{H}_2\text{O}$ ,  $\text{AgNO}_3$ ,  $\text{Mn}(\text{NO}_3)_2 \cdot 4\text{H}_2\text{O}$ ,  $\text{Na}_2\text{S} \cdot 9\text{H}_2\text{O}$ ) were purchased from Sigma-Aldrich and used without further purification.

Two typical quaternary microemulsions consisting of *n*-heptane as organic phase, cetyltrimethylammonium bromide (CTAB) as surfactant, *n*-butanol as cosurfactant and aqueous solutions of the metallic precursor and precipitation agent ( $\text{Na}_2\text{S}$ ), respectively, were prepared. To obtain stable and transparent microemulsions [22], we established the following parameters:  $w_o = 18$  (where  $w_o$  is water/surfactant molar ratio) and *n*-heptane/*n*-butanol = 12/7 (vol.). The microemulsion containing the precipitating agent was mixed in stoichiometric proportions with the metallic precursor microemulsion and the resulting colloidal solution was kept under vigorous stirring at 40 °C for 2 h. In the case of doped cadmium sulfide samples, 0.2 M aqueous solutions of the metallic precursors in the corresponding molar ratios were used.

The colloidal systems were investigated by UV-vis (Able Jasco V560) and photoluminescence (PL) spectroscopy (Perkin Elmer LS55). In order to obtain PL spectra, all samples were irradiated at the wavelength corresponding to the maximum of the excitation spectra ( $\text{CdS}$  391 nm;  $\text{ZnS}$  312 nm;  $\text{Zn}_{0.5}\text{Cd}_{0.5}\text{S}$  381 nm;  $\text{Ag}_{0.1}\text{Cd}_{0.9}\text{S}_{1-x}$  485 nm;  $\text{Cd}_{0.9}\text{Mn}_{0.1}\text{S}$  357 nm). To isolate pure and doped cadmium sulfide nanoparticles from the corresponding microemulsion system, the solvents were evaporated and the chalcogenide nanocrystals were intensively washed with water and ethanol and separated by centrifugation. The obtained nanocrystals were investigated by X-ray diffraction (XRD) performed on a Rigaku Miniflex II using  $\text{CuK}\alpha$  radiation, scanning with 0.01°/step, at 2°/min speed, and by scanning and transmission electron microscopy using Tescan Vega III scanning electron microscope and Tecnai G<sup>2</sup> F30 S-TWIN high resolution transmission electron microscope, respectively. The elemental composition of doped sulfides was determined by energy dispersive X-ray spectroscopy (EDX) associated with SEM.

## 3. Results and discussion

The isolated pure and doped cadmium sulfide nanoparticles were structural analyzed by XRD. For a comprehensive study of zinc doped cadmium sulfide,  $\text{ZnS}$  nanoparticles were also synthesized by the same method. Fig. 1 presents the XRD patterns of pure  $\text{CdS}$ ,  $\text{Cd}_{0.5}\text{Zn}_{0.5}\text{S}$  and  $\text{ZnS}$  prepared from metallic chlorides.

$\text{CdS}$ ,  $\text{Cd}_{0.9}\text{Mn}_{0.1}\text{S}$  and  $\text{Cd}_{0.9}\text{Ag}_{0.1}\text{S}_{1-x}$  samples obtained from cadmium acetate and the corresponding aqueous solutions of the doping ion, manganese nitrate and silver nitrate, respectively, were also investigated by X-ray diffraction (Fig. 2). All the samples are single phase compounds with cubic symmetry, except for the case of silver doped cadmium sulfide. XRD

patterns of  $\text{Cd}_{0.9}\text{Ag}_{0.1}\text{S}_{1-x}$  reveal the formation of a mixture of cubic and hexagonal cadmium sulfide, as well as of  $\text{Ag}_2\text{S}$  as secondary phase. Table 1 lists the lattice parameters and the crystallite size,  $D_{220}$ , of the obtained sulfide nanoparticles, calculated with Rigaku PDXL software. It has been noticed that the cell volume decreases for  $\text{Mn}^{2+}$  and  $\text{Zn}^{2+}$  doped samples, in agreement with smaller ionic radii of doping ions than of  $\text{Cd}^{2+}$ . The synthesized nanoparticles present sphalerite structure with cubic symmetry, but the XRD patterns indicate also the formation of a small content of hexagonal phase. XRD data for zinc and manganese doped cadmium sulfide proved the accommodation of zinc and manganese ions in the crystalline lattice of cadmium sulfide.

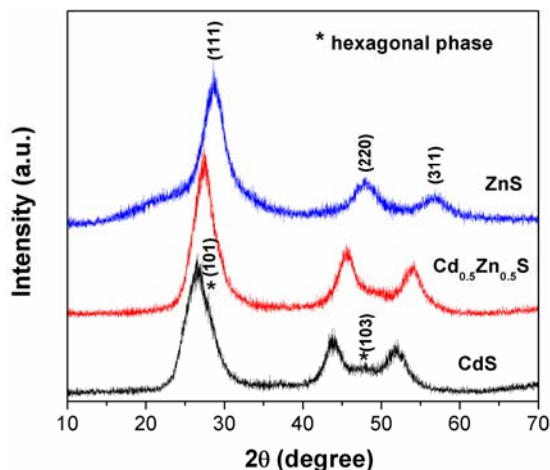


Fig. 1. XRD patterns of CdS,  $\text{Cd}_{0.5}\text{Zn}_{0.5}\text{S}$  and ZnS synthesized from the corresponding metallic chlorides.

Table 1. Some structural properties of sulfide samples.

Compound	Precursor anion	$a$ ( $\text{\AA}$ )	$V$ ( $\text{\AA}^3$ )	$D_{220}$ (nm)
CdS	chloride	5.805	195.65	2
CdS	acetate	5.866	201.88	3
$\text{Cd}_{0.9}\text{Mn}_{0.1}\text{S}$	acetate, nitrate	5.855	200.71	2
$\text{Cd}_{0.5}\text{Zn}_{0.5}\text{S}$	chloride	5.584	174.18	4
ZnS	chloride	5.336	151.90	3

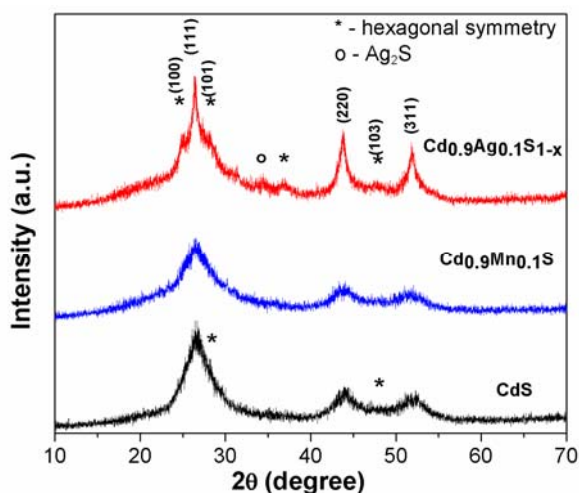


Fig. 2. XRD patterns of pure and doped cadmium sulfide samples obtained from the corresponding metallic acetates and nitrates.

The UV-vis spectra of CdS, ZnS and  $\text{Cd}_{0.5}\text{Zn}_{0.5}\text{S}$  colloidal systems are illustrated in Fig. 3A. All colloids present a broad and blue shifted absorption band in comparison with the corresponding bulk compounds, asserting the formation of nanosized particles, in agreement with literature data [23].

Cadmium sulfide nanocrystals exhibited weak photoluminescence ( $I = 15$  a.u., where  $I$  stands for PL intensity) with a maximum emission at 528 nm (Fig. 3B, black curve), whereas zinc sulfide sample presented an intense emission ( $I = 10500$  a.u.) at 365 nm (Fig. 3B, blue curve). As for  $\text{Cd}_{0.5}\text{Zn}_{0.5}\text{S}_{1-x}$ , the PL spectra revealed an enhanced ( $I = 3900$  a.u.) wide Gaussian emission band centered at 529 nm, resembling the maximum emission peak of pristine cadmium sulfide (Fig. 3B, red curve). The intense luminescence in the visible range of  $\text{Cd}_{0.5}\text{Zn}_{0.5}\text{S}$  colloid under irradiation with a UV lamp at 360 nm, it is evidenced in the picture (Fig. 4A). The bright white light emission of zinc-doped cadmium sulfide recommends this compound as phosphor for white LEDs fabrication.

The presence of silver ions in cadmium sulfide colloidal system led to an increase of the photoluminescence of pristine compound and shifted the emission peak towards higher wavelength, from 507 to 611 nm (Fig. 4B, red curve). The colloidal system of silver-doped cadmium sulfide presented red emission in visible spectrum, although the solid powder is brown because of silver sulfide phase segregation. Unlike silver and zinc doped cadmium sulfide, presence of  $\text{Mn}^{2+}$  ions as dopant in cadmium sulfide colloid did not alter significantly the photoluminescence (Fig. 4B, blue curve). A weak emission centered on 605 nm can be noticed and it could be assigned to  ${}^4\text{T}_1 \rightarrow {}^6\text{A}_1$  transition of  $\text{Mn}^{2+}$  ions in tetrahedral coordination in the lattice of  $\text{Cd}_{0.9}\text{Mn}_{0.1}\text{S}$  [21].

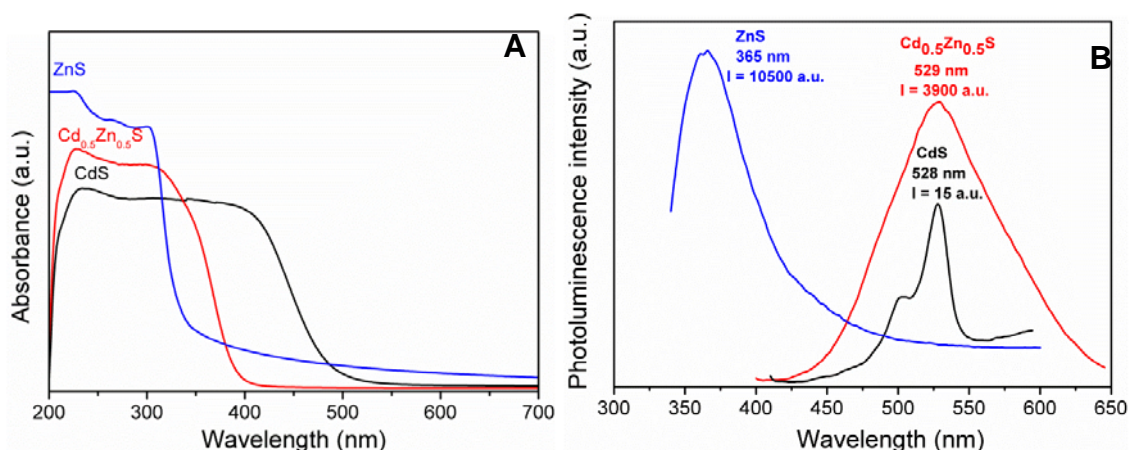


Fig. 3. UV-vis spectra (A) and normalized PL spectra (B) of CdS,  $\text{Cd}_{0.5}\text{Zn}_{0.5}\text{S}$  and ZnS.

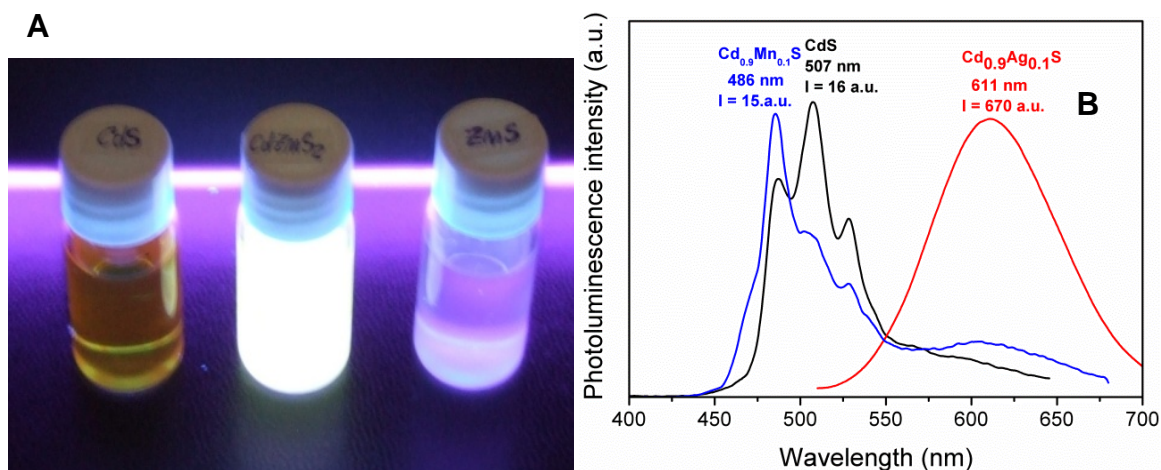


Fig. 4. From left to right: CdS,  $\text{Cd}_{0.5}\text{Zn}_{0.5}\text{S}$  and ZnS samples under UV irradiation (A); Normalized PL spectra of CdS,  $\text{Mn}_{0.1}\text{Cd}_{0.9}\text{S}$  and  $\text{Cd}_{0.9}\text{Ag}_{0.1}\text{S}$  (B).



The isolated pure and doped cadmium sulfide nanoparticles were morphologically investigated by scanning and transmission electron microscopy (Fig. 5-7). The SEM investigation showed that sulfide nanoparticles had the tendency to form spherical agglomeration in the range of 50-200 nm in the case of CdS (Fig. 5A) and 50-100 nm for  $\text{Cd}_{0.5}\text{Zn}_{0.5}\text{S}$  sample (Fig. 6A). All metallic chalcogenide samples prepared by reverse microemulsion method presented very small, spherical particles with narrow size distribution, in the range of 3-5 nm as TEM investigation showed. The particles dimension from TEM analysis matched well with the determined crystallite size values calculated from XRD patterns (Table 1). Selected area electron diffraction patterns (SAED) indicated that the crystal structure of ZnS and CdS nanoparticles was cubic, in agreement with X-ray diffraction data. The small particle size of CdS caused the observed diffuse electron diffraction rings pattern (Fig. 5B inset). The chemical composition of the prepared samples was determined by energy dispersive X-ray microanalysis coupled with scanning electron microscope. Chemical compositions with values very similar to the theoretical ones were obtained (e.g. for CdS and  $\text{Cd}_{0.5}\text{Zn}_{0.5}\text{S}$ , the molar ratio Cd:S=1:1.02 and Cd:Zn:S=0.5:0.52:0.98, respectively).

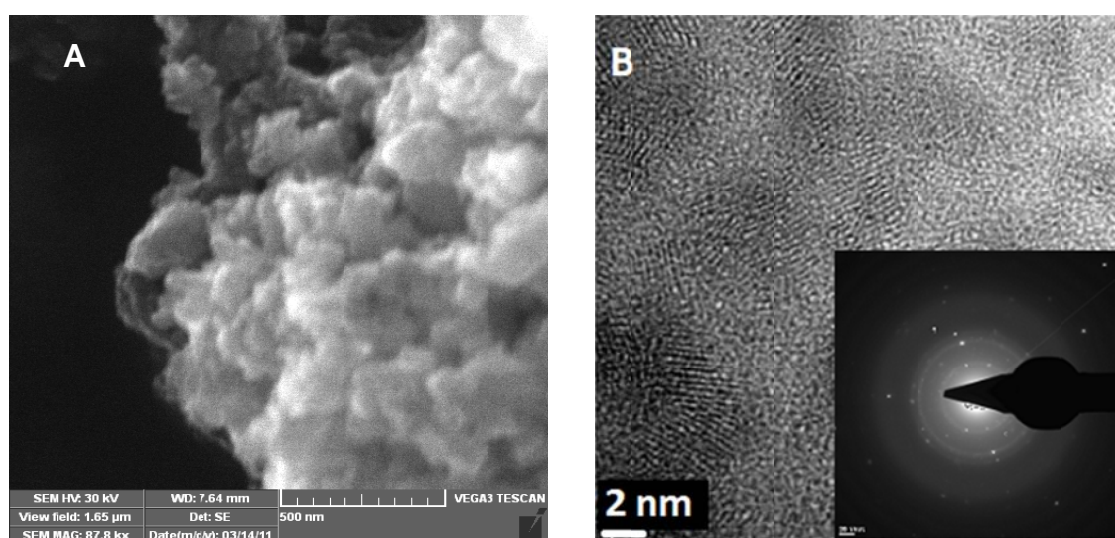


Fig. 5. SEM micrograph (A) and HRTEM image (inset - SAED image) (B) of CdS.

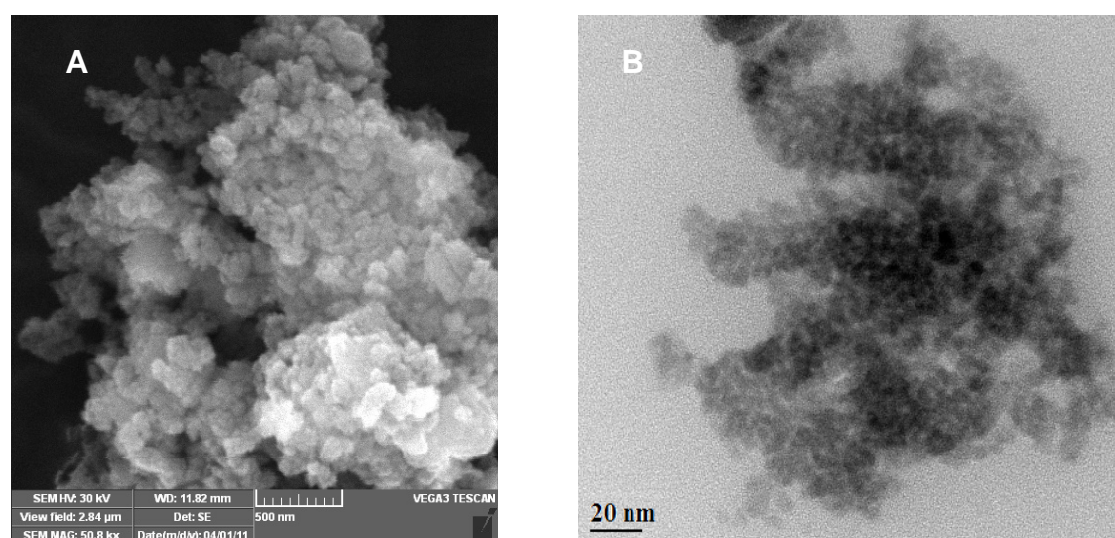
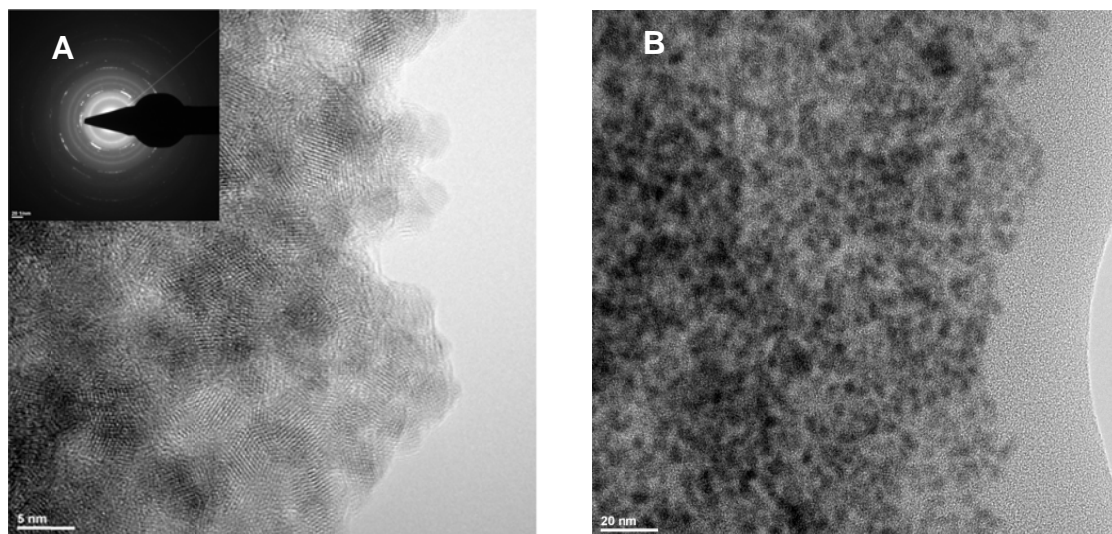


Fig. 6. SEM micrograph (A) and TEM image (B) of  $\text{Cd}_{0.5}\text{Zn}_{0.5}\text{S}$ .

Similar morphology was observed on HRTEM analysis for ZnS sample prepared by reverse microemulsion method in the same conditions as CdS. The particles size of ZnS sample

was in the range of 3-5 nm (Fig. 7A). Also, for the manganese-doped cadmium sulfide sample, TEM analysis demonstrated the formation of small spherical, well-dispersed nanoparticles with a very narrow size distribution, with same size as the pristine compound (Fig. 7B).



*Fig. 7. HRTEM image of ZnS (inset - SAED pattern) (A); TEM micrograph of Cd<sub>0.9</sub>Mn<sub>0.1</sub>S (B).*

#### 4. Conclusions

The influence of different dopant ions on the photoluminescence of cadmium sulfide nanocrystals was studied. Metallic sulfide nanoparticles with very narrow size distribution were synthesized by double reverse microemulsion method, a very important issue when compounds with size depending properties are compared. A two order enhancement of the photoluminescence in the case of doped Zn<sup>2+</sup> and Ag<sup>+</sup> samples was observed, comparing with pristine cadmium sulfide. Cd<sub>0.5</sub>Zn<sub>0.5</sub>S had the photoluminescence maximum at the same wavelength as CdS, whereas Ag<sup>+</sup> doped sample exhibited a clear red shift of the maximum. For Mn<sup>2+</sup> doped cadmium sulfide, a very similar PL spectrum with the one of pure CdS was measured.

#### Acknowledgment

The financial support of the Romanian project PCCA no.131/2012 is gratefully acknowledged.

#### References

- [1] J. Zhang, Y. Tang, K. Lee, M. Ouyang, *Nature* **466**, 91(2010).
- [2] K. Singh, N.K.Verma, H.S. Bhatti, *Physica B* **404**, 300 (2009).
- [3] A.L. Carabat, D. Berger, S. Georgescu, S. Nastase, S. Stoleriu, C. Matei, *Rev. Rom. Mat.* **43**, 294 (2012).
- [4] A.M. Voiculescu, S. Georgescu, S. Nastase, C. Matei, D. Berger, C. Matei, A. Stefan, O. Toma, *J. Sol-Gel Sci. Technol.* **64**, 667 (2012).
- [5] T. Zuo, Z. Sun, Y. Zhao, X. Jiang, X. Gao, *J. Am. Chem. Soc.* **132**, 6618 (2010).
- [6] S. Shen, L. Guo, *Mater. Res. Bull.* **43**, 437 (2008).
- [7] S. Antohe, V. Ghenescu, S. Iftimie, A. Radu, O. Toma, L. Ion, *Dig. J. Nanomater. Bios.* **7**, 941 (2012).
- [8] I. Willner, R. Baron, B. Willner, *Biosens. Bioelectron.* **22**, 1841 (2007).
- [9] D.R. Jung, J. Kim, S. Nam, C. Nahm, H. Choi, J.I. Kim, J. Lee, C. Kim, B. Park, *Appl. Phys. Lett.* **99**, art. no. 041906 (2011).

- [10] Q. Huo, Colloids Surf. B: Biointerfaces **59**, 1 (2007).
- [11] J. Wang, Y. Shan, W.W. Zhao, J.J. Xu, H.Y. Chen, Anal. Chem. **83**, 4004 (2011).
- [12] G. Jie, B. Liu, H. Pan, J.J. Zhu, H.Y. Chen, Anal. Chem. **79**, 5574 (2007).
- [13] J. Wang, W.W. Zhao, H. Zhou, J.J. Xu, H.Y. Chen, Biosens. Bioelectron. **41**, 615 (2013).
- [14] J. Park, J. Joo, S.G. Kwon, Y. Jang, T. Hyeon, Angew. Chem. Int. Ed. **46**, 4630 (2007).
- [15] D. Chen, L. Gao, Solid State Commun. **133**, 145 (2005).
- [16] E. Caponetti, D.C. Martino, M. Leone, L. Pedone, M.L. Saladino, V. Vetri, J. Colloid Interface Sci. **304**, 413 (2006).
- [17] X. Fu, D. Wang, J. Wang, H. Shi, C. Song, Mater. Res. Bull. **39**, 1869 (2004).
- [18] A.M. Fontes Garcia, M.S.F. Fernandes, P.J.G. Coutinho, Nanoscale Res. Lett. **6**, art. no. 426, 1 (2011).
- [19] M. Romcevic, N. Romcevic, R. Kostic, L. Klopotoski, W.D. Dobrowolski, J. Kossut, M.I. Comor, J. Alloys Compd. **497**, 46 (2010).
- [20] R. Sathyamoorthy, P. Sudhagar, A. Balerna, C. Balasubramanian, S. Bellucci, J. Alloys Compd. **493**, 240 (2010).
- [21] S. Arora, S.S. Manoharan, Solid State Commun. **144**, 319 (2007).
- [22] J. Eastoe, M.J. Hollamby, L. Hudson, Adv. Colloid Interface Sci. **128–130**, 5 (2006)
- [23] P. Verma, G.S. Manoj, A. C. Pandey, Physica B **405**, 1253 (2010).